Analysis of power-dependent switching between radiatively coupled planar waveguides

M. Shamonin, M. Lohmeyer and P. Hertel

Abstract— **Effective coupling between two remote optical waveguides without branching sections can be achieved in a three-guide system with multimode central waveguide. We investigate the nonlinear power switching of c.w. laser radiation by such radiatively coupled waveguides. It is shown that effective all-optical switches with spatially well separated input/output channels can be realized although the influence of multimode interference on the switching characteristics becomes more pronounced for increasing thickness of the central guide. Different coupling regimes are specified, and the changes in switching characteristics during the transformation from one regime to another is studied. Numerical calculations for the critical power are compared with an approximate analytical expression. It is also shown that, at a moderate input power, a small number of modes determines the switching behaviour.**

Keywords— **integrated optics, nonlinear directional coupler, radiatively coupled waveguides, power-dependent switch**

I. Introduction

Directional couplers (DC) are important components for a number of integrated optical applications [1]. Conventional couplers rely on the overlap of evanescent fields outside the guiding regions. Alternatively, the leaky modes of isolated waveguides can be used to achieve the radiation transfer. The latter principle is called radiative coupling. Examples are antiresonant reflecting optical waveguides (ARROW) [2], [3], coupled corrugated waveguides [4], [5], and leaky anisotropic waveguides [6]. The big advantage of the radiatively coupled DC is that the coupling length does not increase exponentially with the waveguide separation. This allows to design DC without branching sections but with good separation of the optical channels.

Nonlinear directional couplers (NLDC) are promising components for the realization of ultrafast all-optical switches and logic gates [7], [8], [9], [10]. A typical device comprises two optical channels. In power-controlled switches the output is a function of the input power launched into one channel. The proposed power-dependent switches with spatially well separated optical channels are based on so-called soliton couplers [11] or on ARROW-structures [12], [13]. The soliton coupler requires an extremely large and at present not-available nonlinearity. The ARROW-structure consists of many layers, the thickness and refractive index of which must be accurately controlled.

Motivated by the research reported in [12], [13] we investigate in detail a nonlinear directional coupler based on radiatively coupled (RC) planar waveguides [14], [15] (see Fig. 1). The concept of radiatively coupled planar waveguides is briefly reviewed in section II. Section III is devoted to nonlinear switching between RC waveguides. A theory using the linear normal modes of the entire structure (supermodes) is presented and numerically verified in subsections III-A and III-B, respectively. It is a generalization of the approach by Silberberg and Stegeman [16]. The properties of the proposed NLDC are discussed in subsection III-C. Section IV summarizes the conclusions.

The authors are with the Department of Physics, University of Osnabrück, Barbarastraße 7, D-49069 Osnabrück, Germany

Figure 1

Fig. 1. Nonlinear directional coupler based on radiatively coupled planar waveguides. The three-guide coupler consists of two monomode waveguides (refractive index n_1, guide thickness h) separated by the buffer layer (refractive index n_2) of thickness t from the central waveguide (refractive index n_3, thickness H). The surrounding has the refractive index n_0. The hatched regions are made of nonlinear optical materials with the same value χ of the nonlinear coefficient . The variation of the refractive index in the cross-section is shown. β^* denotes the propagation constant of the mode of the isolated outer waveguides.

II. Linear radiatively coupled waveguides

The structure of interest is shown in Figure 1. It consists of two monomode outer slab waveguides, denoted as WG1 and WG2, and a third multimode waveguide between them. Such an arrangement is often called 'radiatively coupled waveguides' since it can be considered as a system of two leaky waveguides sharing a common substrate [14]. The most interesting feature of such a system is that the light launched into one outer waveguide, say WG1, will be transferred to the other waveguide WG2, after a certain distance called the coupling length L_c, even if the outer optical channels WG1 and WG2 are spatially well separated. Reported potential applications of RC waveguides are the remote coupler [14], an integrated optical sensor [17], a TE/TM polarization splitter [15], and an integrated optical circulator [18].

If the mode of an isolated outer waveguide with the propagation constant β^* is used for an excitation, the characteristic coupling length L_c can be determined from the propagation constants β_s, β_a of the two (symmetric s, antisymmetric a) modes of the entire system, which are closest to β^*:

$$L_c = \frac{\pi}{|\beta_s - \beta_a|} . \qquad (1)$$

Although definition (1) is similar to the well-known case of conventionally coupled waveguides, the pertinent modes are in general not the fundamental modes of the entire structure.

Figure 2

Fig. 2. Dependence of the effective mode indices β/k_0 and of the coupling length L_c on the central guide thickness H. a and b denote two examples for the three- and two-mode regimes, respectively. Parameters: $n_0 = n_2 = 1.55$, $n_1 = n_3 = 1.57$, $h = 2$ μm, $t = 1.7$ μm and $\lambda = 1.064$ μm [19].

Since the refractive index of the central waveguide is larger than the effective mode indices, the mode fields oscillate in the central waveguide. This leads to the almost periodical dependence of the propagation constants and of the coupling length on the thickness H of the central waveguide as shown in Figure 2. The dispersion characteristics are remarkably similar to those of an ARROW coupler[2]. Depending on the value of H, mainly two or three modes, with propagation constants closest to β^* determine the propagation behaviour. The two-mode regime (two modes dominate) appears in the vicinity of the local maxima of the $L_c(H)$-dependence while the three-mode regime (three modes dominate) corresponds to the local minima of the $L_c(H)$ graphs. These regimes were first identified in Ref. [13]. An example is marked in Figure 2, and the corresponding mode field profiles are depicted in Figure 3. It turns out that at the distance of L_c best conditions for complete power transfer between the outer waveguides occur in the two- or three-mode regime. In the following we investigate the power-dependent switching in such a system of two RC waveguides. TE-polarized fields are considered, and only the waveguides proper are assumed to be realized with nonlinear material.

Figure 3

Fig. 3. Mode field profiles corresponding to three- (a) and two-mode regimes (b) marked in Fig. 2

III. Nonlinear switching

A. Theory

We represent the principal electric field component as a superposition of guided modes of the entire linear structure,

$$E_y(x,z) = \sum_{p=1}^{N} a_p(z)\mathcal{E}_p(x)\exp[-\mathrm{i}\beta_0 z]\,, \qquad (2)$$

where β_0 is a reference propagation constant and N is the total number of guided modes. The real mode field profile $\mathcal{E}_p(x)$ is normalized as $(2\omega\mu_0)^{-1}\beta_0\int\mathcal{E}_p^2 dx = 1$. The expansion coefficients a_p become coupled due to the presence of the nonlinear polarization. If the nonlinear coupling is small, these amplitudes vary but slowly. The resulting nonlinear system of equations is

$$\mathrm{i}\frac{\partial a_p}{\partial z} = B_p a_p + \sum_{qrs} C_{pqrs} a_q a_r a_s^* \qquad p = 1,\ldots,N\,. \qquad (3)$$

In Eq.(3) $B_p = (\beta_p^2 - \beta_0^2)/2\beta_0$ and $C_{pqrs} = (\omega\epsilon_0/4)\times\int\chi(x)\,\mathcal{E}_p\mathcal{E}_q\mathcal{E}_r\mathcal{E}_s\,dx$ where $\chi(x)$ is the nonlinear coefficient related to the nonlinear susceptibility tensor, ω the angular frequency and β_p the propagation constant of p-th mode. If $\beta_0 \approx \beta_p$ for all relevant modes, one can set $B_p = \beta_p - \beta_0$ [20]. With the latter approximation it is easily seen that in the linearity limit $\chi = 0$ the system (3) describes the multimode interference in the usual way. In the following analysis we use $\beta_0 = \beta^*$. Since the structures of interest are weakly guiding ($\beta^* \approx \beta_p$) this approximation is justified. Moreover, $\mathcal{P}_p = |a_p|^2$ can be interpreted as the power transported by the p-th mode. It is important that the system of equations (3) is conservative: $\partial_z\left(\sum_p \mathcal{P}_p\right) = 0$.

B. Numerical verification

The system (3) was solved using the variable-order variable-step Adams method with the routines of the NAG Fortran library [21]. Initial conditions were assumed according to the typical experimental situation such as in Ref. [14], namely the fundamental mode $\sqrt{P_{\mathrm{in}}}\Psi_1(x)$ of the isolated outer waveguide WG1 was launched into the coupler at port A (see Fig. 1). Here P_{in} is the power carried by the mode and $\Psi_1(x)$ its normalized field profile. The initial values of amplitudes a_p in (3) are found by calculating the corresponding overlap integrals

$$\begin{aligned} a_p(0) &= \sqrt{P_{\mathrm{in}}}\,\langle\Psi_1,\mathcal{E}_p\rangle \\ &= \sqrt{P_{\mathrm{in}}}\cdot\frac{\beta_0}{2\omega\mu_0}\int_{-\infty}^{\infty}\Psi_1(x)\cdot\mathcal{E}_p(x)\,dx\,. \end{aligned} \qquad (4)$$

Since the thickness t of the buffer layer is large, the initial field is very well represented by a superposition (2): $\sum_{p=1}^{N}\mathcal{P}_p \geq 0.9995 P_{\mathrm{in}}$ holds in all our calculations. To calculate the transmissions T_1, T_2 through the 'bar' channel WG1 (output at B) and through the 'cross' channel WG2 (output at C), respectively, one has to take into account the overlap of the output field with the mode field Ψ_{j} of the output channel:

$$T_{\mathrm{j}} = |\sum_{p=1}^{N} a_p(L_c)\,\langle\Psi_{\mathrm{j}},\mathcal{E}_p\rangle\,|^2/P_{\mathrm{in}} \qquad (\mathrm{j}=1,2)\,. \qquad (5)$$

To verify the mathematical analysis (3) and its numerical implementation we compare our results with published findings. In the literature nonlinear directional couplers based on two [9] and three [22], [23], [24] identical waveguides have been discussed. We have chosen the parameters of a recent publication [22] for comparison: $n_0 = n_2 = 1.53$, $n_1 = n_3 = 1.55$, $h = 2$ μm, $t = 3$ μm, $\chi = 6.377\cdot 10^{-12}$ $\mathrm{m^2V^{-2}}$; the two-guide NLDC corresponds to $H = 0$ μm and the three-guide NLDC is characterized by $H = h = 2$ μm. The device length is 1.93 mm and 2.73 mm, respectively. Figure 4 shows the switching characteristics for the two-guide NLDC (a) and for the three-guide NLDC (b). As in [22], the input power is normalized on the characteristic input power $P_{1\max}$, at which the transmission in WG1 takes a first maximum. We obtain $P_{1\max} = 1.84$ W/m and $P_{1\max} = 1.75$ W/m for the two- and three-guide

Figure 4

Fig. 4. Fractional power that exits from WG1 (solid lines) and WG2 (dashed lines) for the two-guide NLDC (a) and for the three-guide NLDC (b) of Ref.[22]. See the text for parameter values.

NLDC, respectively. The curve for the three-guide NLDC is indistinguishable from that obtained in [22] who used a finite-difference beam-propagation method (FD-BPM). As expected, both curves are very close to those obtained by an analysis based on the coupled modes of isolated waveguides, except for slightly larger values of $P_{1\max}$ predicted by the FD-BPM and our method. We conclude that, although consistent with the analysis based on coupled modes of single waveguides, the results obtained by using the coupled supermodes agree better with the FD-BPM calculations. The present approach and the FD-BPM calculations are based on the same SVEA, while the alternative approach involves a singular perturbation technique [22].

C. Results and discussion

In the following we consider the structure of Ref. [19]. Its parameters are $n_0 = n_2 = 1.55$, $n_1 = n_3 = 1.57$, $h = 2.0$ μm, $t = 1.7$ μm, and the operation wavelength $\lambda = 1.064$ μm. H varies from 0 up to 20 μm. The nonlinear coefficient χ is constant in all three cores. The device length equals the coupling length $L_c(H)$. In the following the power quantities are normalized on $P_\chi = (2\omega\mu_0\chi)^{-1}$. A typical value of P_χ for a semiconductor-doped glass waveguides is 3.58 MW/m [12].

The most important characteristics of a NLDC is the critical power $P_{\rm cr}$, and much previous work is devoted to its determination. $P_{\rm cr}$ is commonly defined in systems supporting two interacting modes. For such couplers the effective energy transfer period becomes infinite at critical power [9]. In this case the input power is asymptotically split between the two waveguides and the device acts as a 3-dB splitter. However, the structure of interest supports several guided modes. We thus define $P_{\rm cr}$ as the smallest input power at which the transmission in the 'bar' (parallel) output channel reaches $T_1 = 1/2$. It will be seen below that for the majority of cases $P_{\rm cr}$ has the same physical significance: it is a typical power level required for switching (see Fig. 5). For input powers below the critical power ($P < P_{\rm cr}$) the device acts as a usual linear coupler. At higher values of input power ($P > P_{\rm cr}$) there is effectively no energy transfer between the waveguides. Note that for multi-waveguide systems the switching characteristics are in general not symmetric with respect to the 1/2-level: $T_1 + T_2 \neq 1$. Moreover, $T_1 = 1/2$ and $T_2 = 1/2$ are achieved for different input powers. A fraction of the optical power can be contained in the central waveguide. This may be seen in Fig. 5(b) where half the input power remains in WG1 while the rest is distributed between the other output channel and the central region.

We compare the numerically obtained values of $P_{\rm cr}$ with those calculated from a simplified two-mode model. In the framework of this model one is considering the nonlinear

Figure 5

Fig. 5. TE-field propagation along the coupler for different input powers: $P_{\rm in} = 0.01\ P_{\rm cr}$ (a), $P_{\rm in} = P_{\rm cr}$ (b), $P_{\rm in} = 1.4\ P_{\rm cr}$ (c). $H = 12.44$ μm, the remaining parameters are as in Fig. 2. The coupler length L_c is 1.225 mm. For a better presentation the input field amplitudes have been scaled to the same level.

interaction of only two modes with propagation constants closest to β^*. (Note that the same modes are used to determine the coupling length.) In this case an analytical expression for the critical power is available (see [12], [19]).

The critical power, as obtained from the analytical formula is compared with results of the numerical simulation in Figure 6. Although the analytical expression is justified only for the two mode regime, its predictions indicate the trend also in the three mode regime: $P_{\rm cr}$ is larger in the three-mode regime than in the two-mode regime. The dependence of $P_{\rm cr}$ on H is mainly determined by the almost periodical dependence $1/L_c(H)$. The remaining factor $P_{\rm cr} \cdot L_c$ shows a less pronounced dependence on H. To qualitatively explain this fact one might argue that switching occurs when the difference of propagation constants of the most excited linear modes is compensated by the nonlinear differential phase shift between them [13]. Therefore, as a rule of thumb, a linear dependence of the critical power on the difference of these propagation constants is expected.

Figure 6

Fig. 6. Dependence of the normalized critical power $P_{\rm cr}/P_\chi$ on the central guide thickness H. The solid line denotes numerically obtained values, the dashed line corresponds to the two-mode model. Parameters are as in Fig. 2.

The observed oscillations of $P_{\rm cr}(H)$ and jumps of $P_{\rm cr}$ with H are caused by multimode interference. They are outside the scope of the two-mode approximation. The last feature – appearance of jumps in $P_{\rm cr}(H)$ – is also related to the particular definition of $P_{\rm cr}$.

To clarify the origin of these jumps we calculated the switching characteristics for several values of H in the interval from $H = 0.31$ μm to $H = 3.77$ μm. Figure 7 shows the results. The boundary values $H = 0.31$ μm (a) and $H = 3.77$ μm (l) correspond to the maximum positions of the $L_c(H)-$dependence (two-mode regime). At $H = 2.04$ μm (marked as c) a local minimum of $L_c(H)$ is achieved (three-mode regime). In the $P_{\rm cr}(H)$-dependence on top of Fig. 7 black boxes (marked from a to l) designate the values of $P_{\rm cr}$ at thicknesses which were selected for the calculations. The study of changes in the switching behaviour in these points allows to follow the transformation of switching curves from the two-mode to the three-mode regime and vice versa. It is seen that the change of switching characteristics from the two-mode regime to the three-mode regime (a to c) is rather simple: the curve merely shifts in the region of larger input powers. The transfer from the three-mode regime to the two-mode regime (from c to l)is much more complicated: additional local maxima

appear in the $T(P_{\rm in})-$dependence. Due to the numerical determination of $P_{\rm cr}$, the jumps in the $P_{\rm cr}(H)-$dependence appear, when these local maxima cross the level $T_1 = 1/2$. For the situation of Fig. 7 three such jumps are observed: between points d and e, g and h, i and j.

When designing a nonlinear switch based on radiatively coupled waveguides one should carefully select the waveguide parameters, such as the central guide thickness H. The conventional nonlinear switch with characteristics like in cases $a-c$ or l are preferable over cases $d-j$. However, it may be that the unusual characteristics with additional zero transmission at large power (e.g. case f) can be utilized to realize novel optoelectronic devices. The almost periodical dependence of the critical power on H in Fig. 6 shows that the observed regularities are qualitatively valid also for larger central layer thicknesses.

Figure 7

Fig. 7. Numerically obtained values of the normalized critical power $P_{\rm cr}/P_\chi$ for central guide thicknesses 0.31 μm $\leq H \leq$ 3.77 μm, remaining parameters as in Fig. 2. $a-l$ denote different typical cases. The corresponding dependences of transmissions T_1 (solid lines) and T_2 (dashed lines) on the normalized input power $P_{\rm in}/P_\chi$ are shown in the insets below. The level $T_{1,2} = 1/2$ is also given for comparison.

Optimal conditions for power transfer between the outer waveguides in the linear regime are found for thicknesses that correspond to local maxima and minima in $L_c(H)$ [15]. Such conditions also result in switching curves that are near to ideal as compared with other thicknesses H.

We have studied the variation of switching characteristics with the central layer thickness H (see Fig. 8). The parameters of the structures are summarized in Table 1. The numbers '2' and '3' in the third column denote the two- and three-mode regime, respectively. The critical power and the slope of switching characteristics for $P/P_{\rm cr} \sim 1$ do not significantly change for the two-mode regime, but the multimode interference results in growing oscillations of the switching curves with increasing central layer thickness H (see Fig. 8). Although the form of the switching curves in the three-mode regime deteriorates with increasing thickness H, oscillations are less pronounced. This is an advantage over the two-mode regime. For the two-mode regime the critical power $P_{\rm cr}$ increases with growing thickness H, and so does the product $P_{\rm cr}\cdot L_c$. For the three-mode regime $P_{\rm cr}$ decreases, while the product $P_{\rm cr}\cdot L_c$ varies slightly and nonmonotonously. In general the product $P_{\rm cr}\cdot L_c$ is approximately $20-30\%$ larger for the three-mode regime, and the switching behaviour is more sensitive to variations of the layer thicknesses than for the two-mode regime. A simple example of this statement can be found in Figure 7 where a slight variation of H results in a drastic change in switching curves (compare cases c through f). In this paper we do not pursue the study of admissible fabrication tolerances further and restrict ourselves to the latter qualitative remarks.

The system of interest supports many guided modes. By launching the fundamental mode of a single outer waveguide into the system, these modes are excited with different amplitudes, thus carrying different amounts of power. Depending on the regime, mainly two or three modes determine the linear coupling. If the waveguide is nonlinear, the coupling between the modes leads to amplification of initially weakly excited modes and to depletion of initially strong modes. Obviously, in order to obtain the most reliable results, all guided modes have to be included into the theoretical model (3). However, for moderate input powers (up to $3P_{\rm cr}$) it is sufficient to use only some modes in order to calculate reliable switching curves. If we first sort the modes according to the carried power, then our calculations show that four relevant modes with the largest power describe the switching behavior well in both two- and three-mode regimes (see Fig. 9). These four modes initially carry more than 98% of the input power as can be seen from Fig. 10. Note that considering only the two or three most strongly excited modes in the two and three-mode regimes, respectively, will lead to overoptimistic conclusions with respect to the switching behavior at large values H.

Figure 8

Fig. 8. Dependence of the transmission T_1 trough the 'bar' channel on the normalized input power $P_{\rm in}/P_{\rm cr}$ in two- (a) and three-mode (b) regimes for different thicknesses H of the central guide: (a) 0.31 μm (solid line), 10.71 μm (dashed line), 14.18 μm (dash-dotted line), 17.65 μm (dotted line); (b) 2.04 μm (solid line), 12.44 μm (dashed line), 15.905 μm (dash-dotted line), 19.37 μm (dotted line). See the text for remaining parameters. The corresponding values of $P_{\rm cr}$ are given in Table 1.

TABLE I

PARAMETERS OF NLDC BASED ON RC WAVEGUIDES OPERATING IN TWO- AND THREE-MODE REGIMES

H [μm]	Regime	N	L_c [mm]	$P_{\rm cr}/P_\chi$	$(P_{\rm cr}/P_\chi)\cdot L_c$ [mm]
0.31	2	3	3.315	0.02430	0.0806
2.04	3	3	0.630	0.18902	0.1190
3.77	2	4	3.369	0.02574	0.0867
5.51	3	5	0.874	0.12878	0.1126
7.24	2	6	3.423	0.02637	0.0903
8.975	3	7	1.064	0.10497	0.1117
10.71	2	7	3.476	0.02734	0.0950
12.44	3	8	1.225	0.09146	0.1121
14.18	2	9	3.528	0.02876	0.1015
15.905	3	10	1.369	0.08473	0.1160
17.65	2	11	3.579	0.02919	0.1045
19.37	3	12	1.501	0.07920	0.1188

IV. Conclusions

Using a three-guide coupler with a multimode central waveguide (radiatively coupled waveguides) a nonlinear power-dependent switch with spatially well separated optical channels can be realized. A theoretical analysis in terms of coupled linear supermodes is proposed. With the help of this model it is shown that best switching character-

Figure 9

Fig. 9. Transmission T_1 through the 'bar' channel versus the normalized input power $P_{in}/P_{\rm cr}$ in two- (a) and three-mode (b) regimes if the two (dashed lines), three (dash-dotted lines) and four (dotted lines) most strongly excited modes are taken into account. Solid lines depict results obtained with all guided modes. Note that the two-mode approximation is not applicable in the three-mode regime (b). Parameters are as in Fig. 2.

Figure 10

Fig. 10. Relative power contained in different mode sets versus the thickness of the central guide. The coupler is excited by the fundamental mode of the isolated outer waveguide. The relative power contained in all guided modes (solid line) is practically unity. The contributions of the two (dashed line), three (dash-dotted line) and four (dotted line) most strongly excited modes are shown. Parameters are as in Fig. 2.

istics are obtained at particular central guide thicknesses where mainly two or three modes determine the propagation pattern (in the linear regime). The transformation of switching characteristics between these regimes has been studied. It is observed that few modes suffice to be considered for moderate input power values. We believe that the new design for a nonlinear directional coupler is promising for applications in integrated all-optical switching devices.

V. Acknowledgements

Financial support by Deutsche Forschungsgemeinschaft (Graduiertenkolleg "Mikrostruktur oxidischer Kristalle" and Sonderforschungsbereich 225) is gratefully acknowledged.

References

[1] T. Tamir, Ed., *Guided-Wave Optoelectronics*. Berlin: Springer-Verlag, (Springer Series in Electronics and Photonics, **26**), pp. 1 - 401, 1988.

[2] M. Mann, U. Trutschel, C. Wächter, L. Leine and F. Lederer, "Directional coupler based on an antiresonant reflecting optical waveguide," Opt. Lett. **16**, 805-807 (1991)

[3] M. Cantin, C. Carignan, R. Cote, M.A. Duguay, R. Larose, P. LeBel and F. Ouelette, "Remotely switched hollow-core antiresonant reflecting optical waveguide " Opt. Lett. **16**, 1738-1740 (1991)

[4] D. Marcuse, "Directional coupler made of nonidentical asymmetric slabs: Part II: Grating-assisted couplers," J. Lightwave Technol. **LT-5**, 268-273 (1987)

[5] V.A. Sychugov, A.V. Tishchenko and B.A. Usievich, "Radiatively coupled corrugated waveguides," Quant. Electron. **21**, 442-444 (1994)

[6] D.V. Petrov, "Directional coupler using a leaky wave of an anisotropic waveguide," IEEE Photon. Technol. Lett. **8**, 381-383 (1996)

[7] S.M. Jensen, "The nonlinear coherent coupler," IEEE J. Quant. Electron. **QE-18**, 1580-1583 (1982)

[8] S. Trillo and S. Wabnitz, "Nonlinear nonreciprocity in a coherent mismatched directional coupler," Appl. Phys. Lett **49**, 752-754 (1986)

[9] G.I. Stegeman and E.M. Wright, "All-optical waveguide switching," Opt. Quant. Electron. **22**, 95-122 (1990)

[10] R.T. Deck and C. Mapalagama, "Improved theory of nonlinear directional coupler," Int. J.of Nonlinear Optical Physics **2**, 43-70 (1993)

[11] D.R. Heatley, E.M. Wright and G.I. Stegeman, "Soliton coupler," Appl. Phys. Lett. **53**, 172-174 (1988)

[12] U. Trutschel, M. Mann, F. Lederer, C. Wächter an A.D. Boardmann, "Nonlinear switching in coupled antiresonant reflecting optical waveguides," Appl. Phys. Lett. **59**, 1940-1942 (1991)

[13] R. Muschall, F. Lederer and U. Trutschel, "New ARROW couplers and switches with significantly reduced coupled length," Int. J. Optoelectron. **8**, 537-546 (1993)

[14] S.M. Loktev, V.A. Sychugov and B.A. Usievich, "Propagation of light in a system of two radiatively coupled waveguides," Quant. Electron. **25**, 435-438 (1994)

[15] M. Shamonin, M. Lohmeyer and P. Hertel, "Directional coupler based on radiatively coupled waveguides," Appl. Opt. **20**(3) (1997) - in print

[16] Y. Silberberg and G.I. Stegeman, "Nonlinear coupling of waveguide modes", Appl. Phys. Lett. **50**, 801-803 (1987)

[17] H. Helmers, P. Benech and R. Rimet, "Integrated optical components employing slab waveguides for sensor applications," IEEE Photon. Technol. Lett.**8**, 81-83 (1996)

[18] M. Lohmeyer, M. Shamonin and P. Hertel, "Integrated optical circulator based radiatively coupled magnetooptic waveguides," Opt. Eng. (1996) - accepted for publication

[19] F. Dios, X. Nogues and F. Canal, "Critical power in a symmetric nonlinear directional coupler," Opt. Quant. Electron. **24**, 1191-1201 (1992)

[20] R.E. Bridges, R.W. Boyd and G.P. Agrawal, "Multidimensional coupling owing to optical nonlinearities. I. General formulation," J. Opt. Soc. Amer. B **13**, 553-559 (1996)

[21] Numerical Agorithms Group Ltd., *NAG Library Manual, Mark 15* (Oxford, 1991)

[22] K. Yasumoto, N. Mitsunaga and H. Maeda, "Coupled-mode analysis of power-transfer characteristics in a three-waveguide nonlinear directional coupler," J. Opt. Soc. Amer. **13**, 621-627 (1996)

[23] Y. Chen, A.W. Snyder and D.J. Mitchell, "Ideal optical switching by nonliner multiple (parasitic) core couplers, Electron. Lett. **26**, 77-78 (1989)

[24] C. Mapalagama and R.T. Deck, "Modified theory of three-channel Kerr-type nonlinear directional coupler," J. Opt. Soc. Amer. A **9**, 2258-2264 (1992)

Figure 1

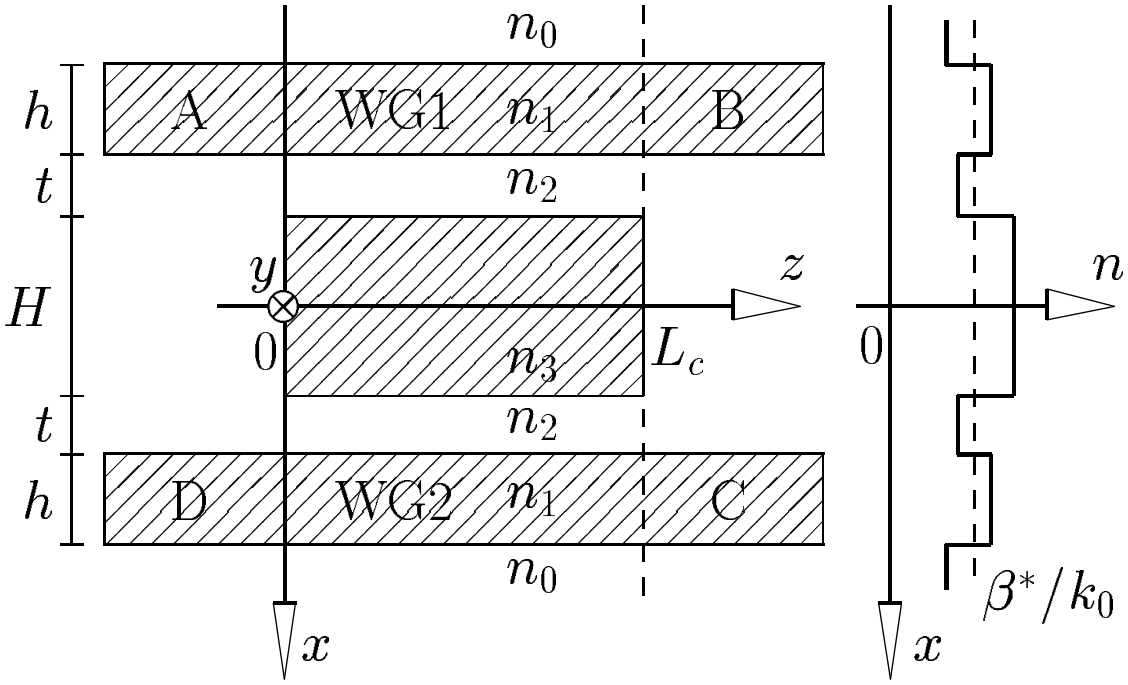

Figure 2

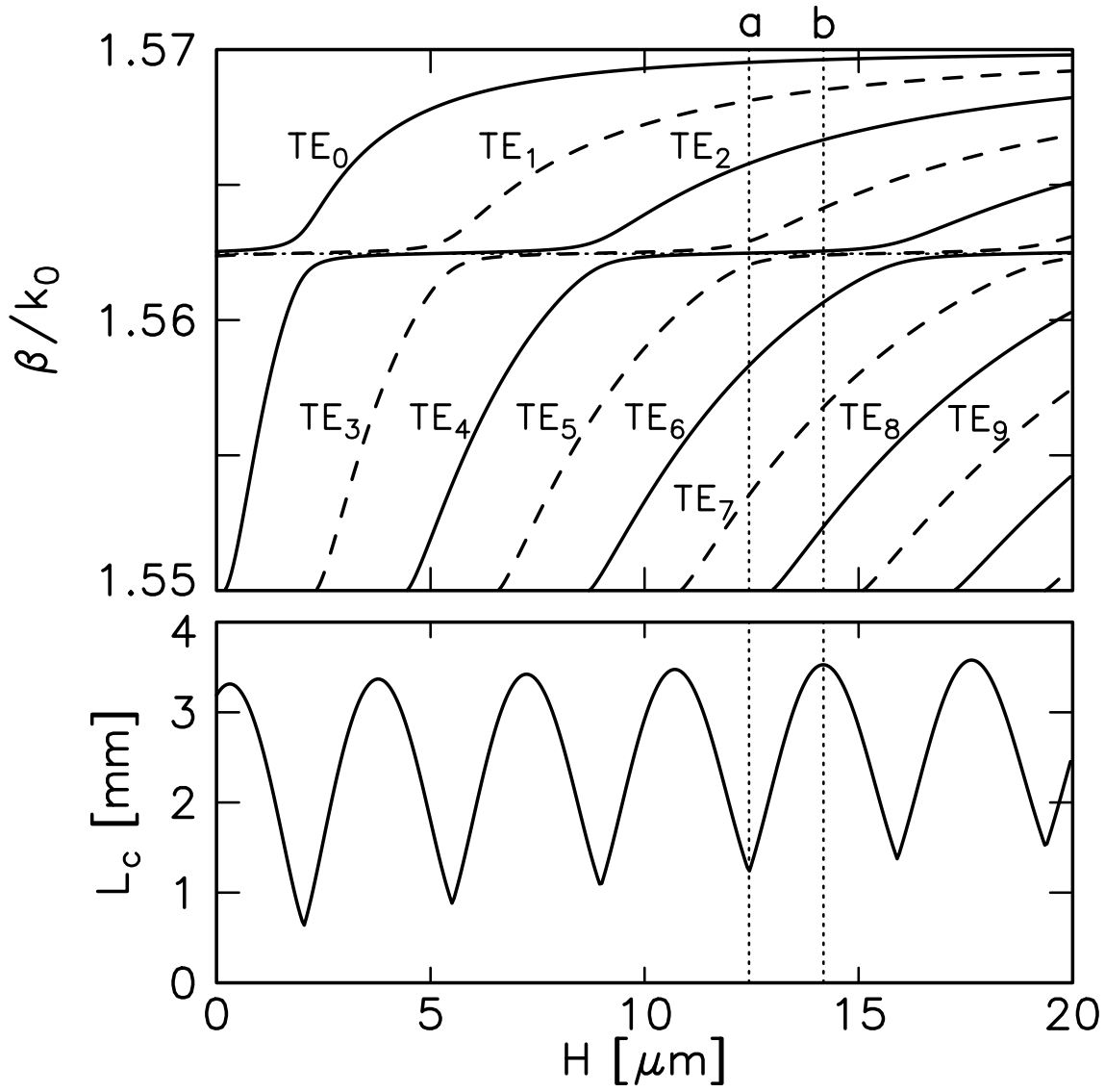
a
b
1.57
1.56
1.55
β/k0
TE0
TE1
TE2
TE3
TE4
TE5
TE6
TE7
TE8
TE9
4
3
2
1
0
Lc [mm]
0
5
10
15
20
H [μm]

Figure 3

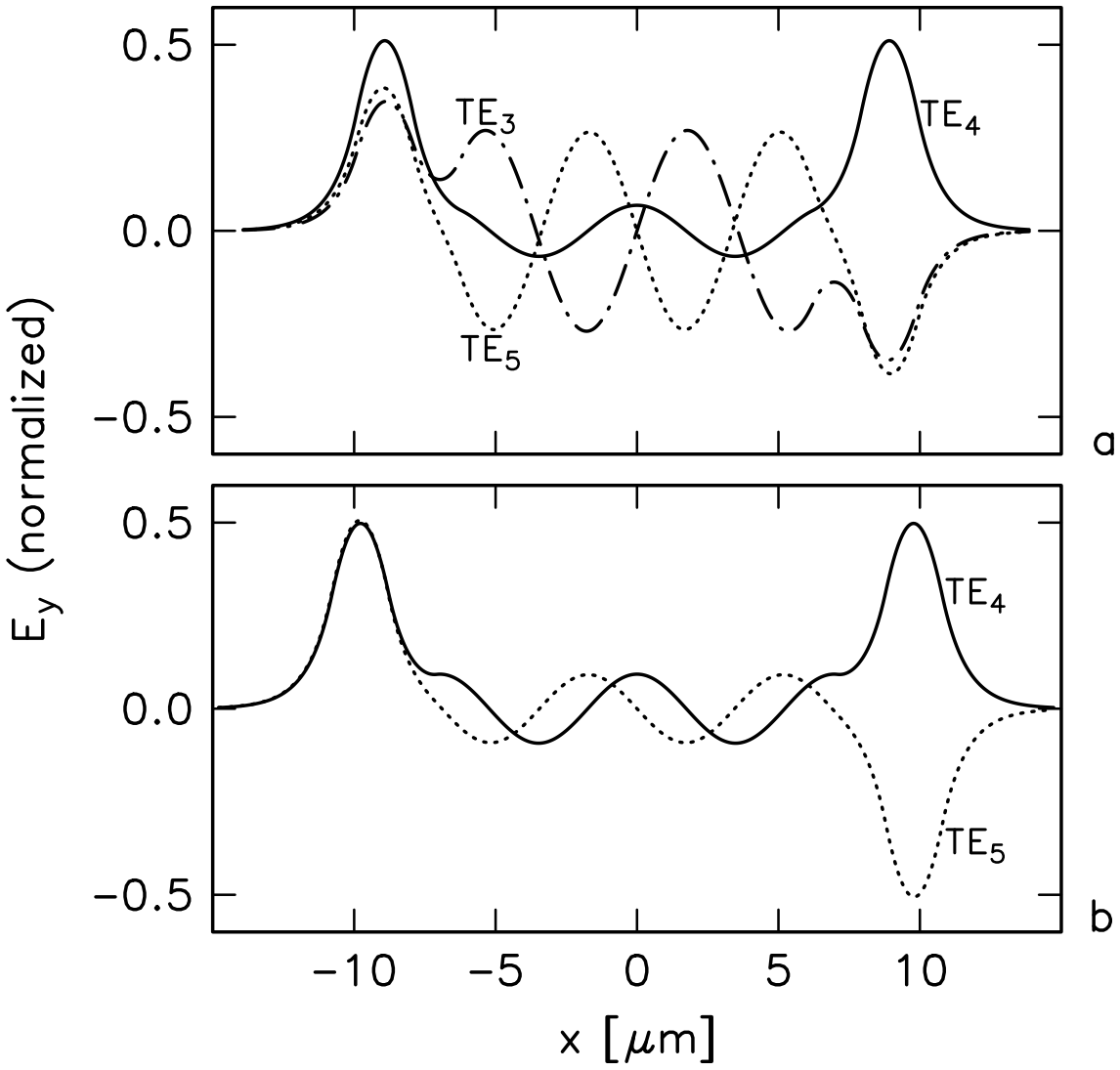
0.5
0.0
−0.5
TE3
TE4
TE5
a
0.5
0.0
−0.5
TE4
TE5
b
−10
−5
0
5
10
x [μm]
Ey (normalized)

Figure 4

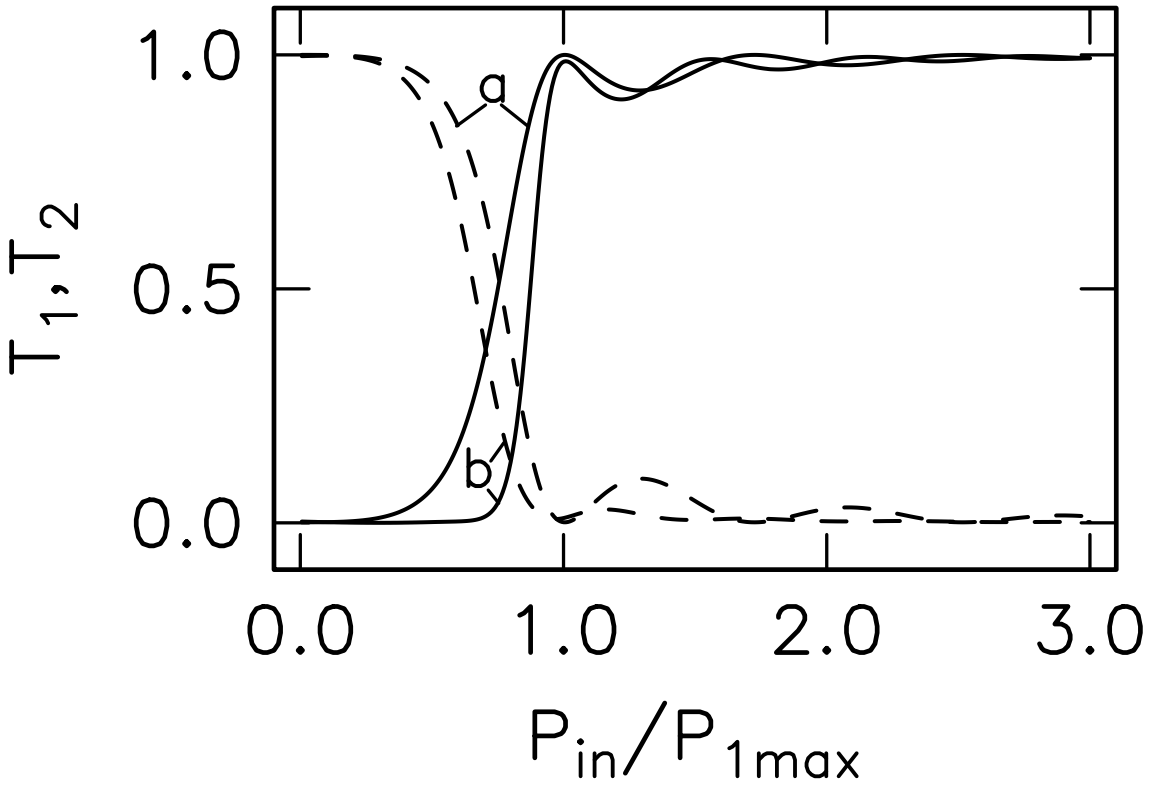

Figure 5

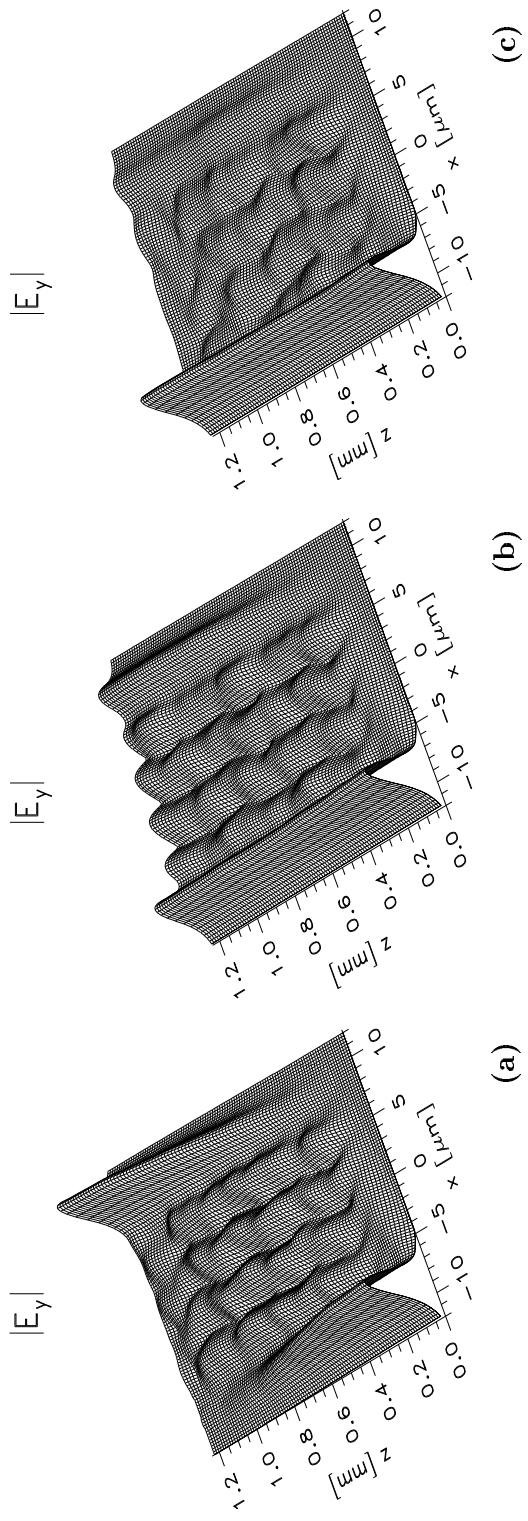

Figure 6

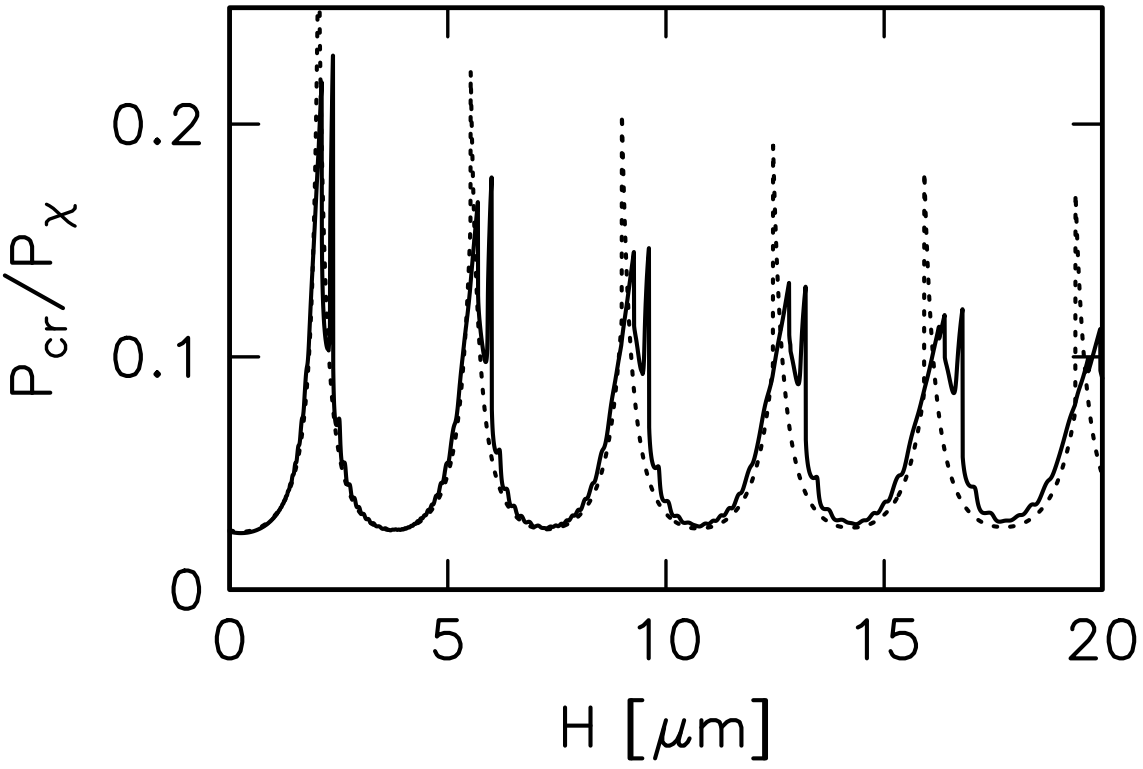

Figure 7

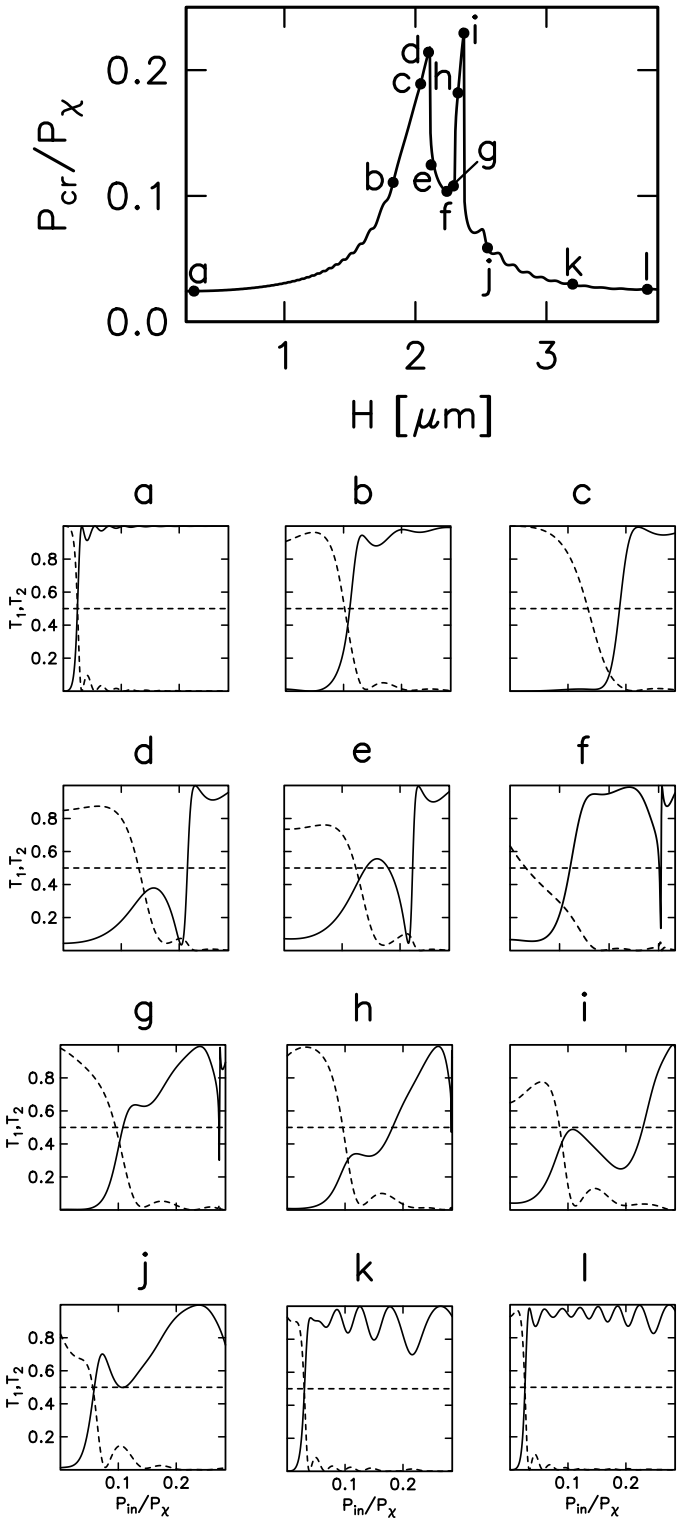
P_{cr}/P_χ
0.0
0.1
0.2
1
2
3
H [μm]
a
b
c
d
e
f
g
h
i
j
k
l
T_1, T_2
0.2
0.4
0.6
0.8
0.1
0.2
P_{in}/P_χ

Figure 8

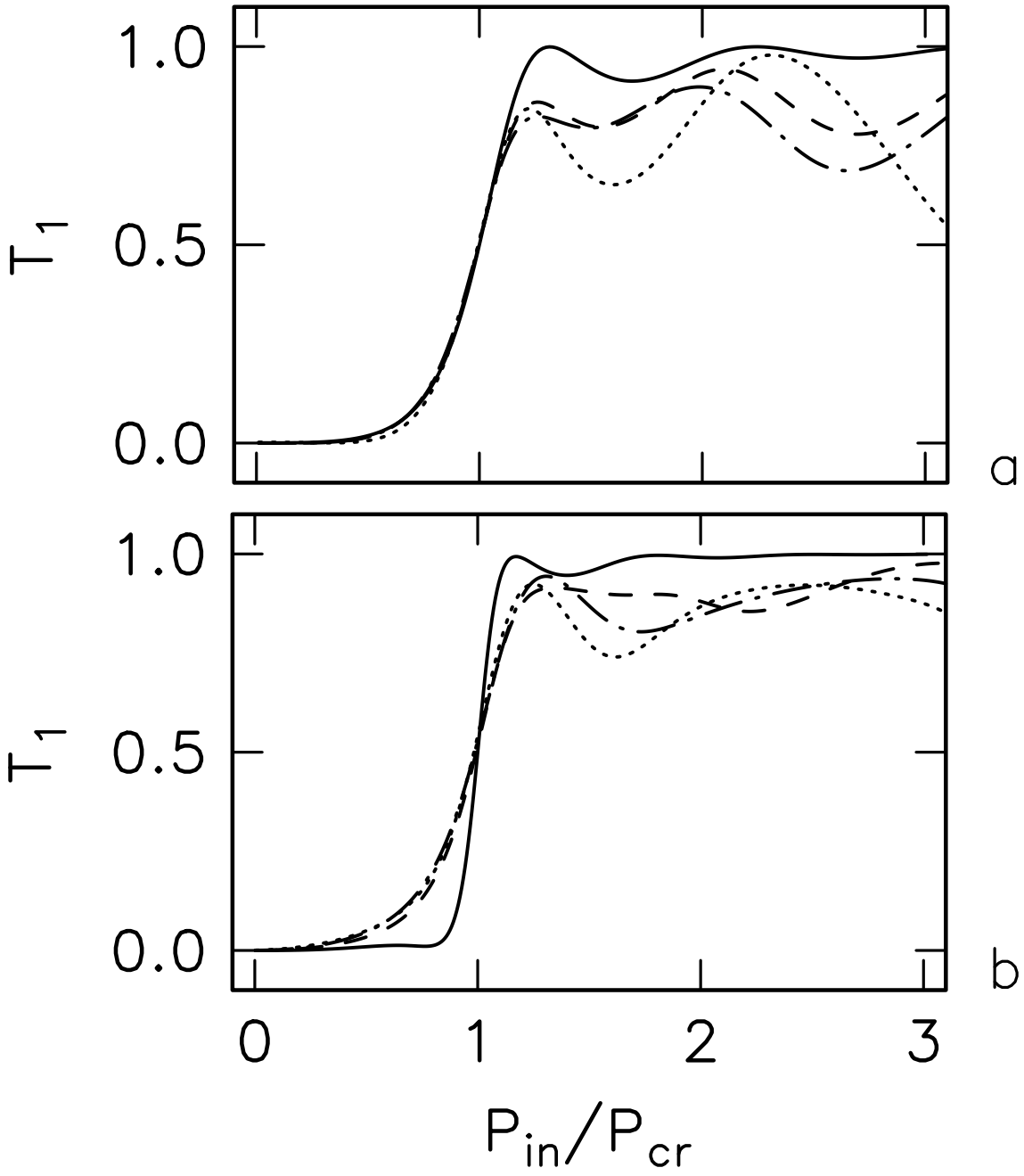

Figure 9

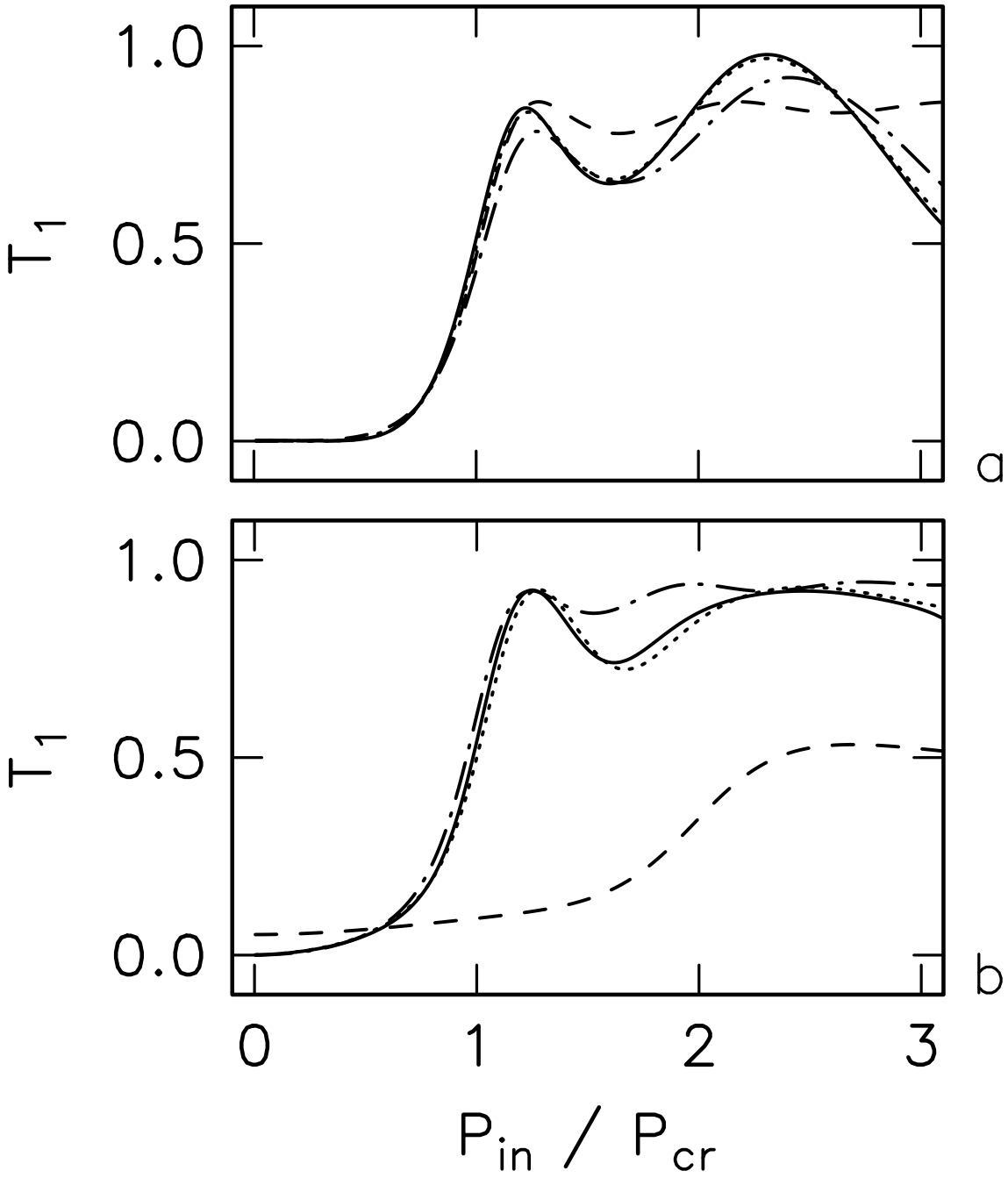

Figure 10